

# Community Detection in General Hypergraph via Graph Embedding

Yaoming Zhen and Junhui Wang  
School of Data Science  
City University of Hong Kong

## Abstract

Conventional network data has largely focused on pairwise interactions between two entities, yet multi-way interactions among multiple entities have been frequently observed in real-life hypergraph networks. In this article, we propose a novel method for detecting community structure in general hypergraph networks, uniform or non-uniform. The proposed method introduces a null vertex to augment a non-uniform hypergraph into a uniform multi-hypergraph, and then embeds the multi-hypergraph in a low-dimensional vector space such that vertices within the same community are close to each other. The resultant optimization task can be efficiently tackled by an alternative updating scheme. The asymptotic consistencies of the proposed method are established in terms of both community detection and hypergraph estimation, which are also supported by numerical experiments on some synthetic and real-life hypergraph networks.

**Keywords:** Latent space model, network embedding, non-uniform hypergraph, sparse network, tensor decomposition

## 1 Introduction

Community detection has attracted increasing attention from both academia and industry in the past few decades, and has a wide spectrum of applications in domains, ranging from social science (Ji et al., 2016; Newman et al., 2002; Zhao et al., 2011; Lee et al., 2017), life science (Chen and Yuan, 2006; Nepusz et al., 2012) to computer science (Tron and Vidal,

2007; Agarwal et al., 2005). The community structure has been widely observed in many real-life networks, which usually means that entities within the same community tend to interact much more often than across communities. In literature, most conventional network analysis focus on pairwise interactions between two vertices (Zhao et al., 2012; Lei et al., 2015; Loyal and Chen, 2020; Sengupta and Chen, 2018). However, the complexity of real-life networks is usually beyond pairwise interaction, and multi-way interactions among vertices arise naturally. For example, in an academic collaboration network, it is often the case that several researches work together on a research project; in a protein-to-protein interaction network, a metabolic reaction usually involves multiple proteins. Under such circumstances, a hypergraph network provides a more faithful representation and retains richer information than a merely vanilla graph network, such as each research project being represented by a hyperedge consisting of multiple vertices being researchers, or each metabolic reaction being a hyperedge consisting of multiple vertices being proteins. In this paper, we are interested in detecting community structure in a hypergraph network, where vertices within the same community share more similar connection patterns compared with vertices in different communities.

To detect communities in a hypergraph network, most existing methods convert the hypergraph into a weighted graph, and then existing graph community detection methods can be applied. For instances, Kumar et al. (2021) defined the hypergraph modularity as the modularity of the weighted graph and applied standard modularity maximization algorithms for community detection, Lee et al. (2021) extended the graph-likelihood-based convex relaxation methods (Li et al., 2020b) on the adjacency matrix of the weighted graph, and Ghoshdastidar and Dukkipati (2017a) conducts spectral clustering on the weighted graph Laplacian for hypergraph community detection. As pointed out in Ke et al. (2021), such conversion will suffer from information loss and lead to suboptimal community detection performance. To circumvent this disadvantage, spiked tensor model (Kim et al., 2017) and

Tensor-SCORE method (Ke et al., 2021) were proposed to conduct community detection on the hypergraph adjacency tensor directly.

Note that most existing hypergraph community detection methods focus on uniform hypergraph only (Ghoshdastidar and Dukkipati, 2014, 2015b; Lee et al., 2021), where all the hyperedges consist of exactly the same number of vertices. When it comes to non-uniform hypergraph, they have to decompose a non-uniform hypergraph into a collection of uniform hypergraphs with different orders, due to the difficulty of lacking an appropriate adjacency tensor for non-uniform hypergraph. It was only until recently that Ouvrard et al. (2021) proposed a heuristic method to construct an adjacency tensor for general hypergraph by adding  $m - m_0$  null vertices, where  $m$  and  $m_0$  are the maximum and minimum cardinality of a hyperedge in the hypergraph, respectively.

In this paper, we propose a novel method for detecting community structure in general hypergraph networks, where a general hypergraph can be uniform or non-uniform. The proposed method consists of an augmentation step and an embedding step. The augmentation step adds a null vertex to the hyperedges with smaller cardinality, and converts the hypergraph into a uniform multi-hypergraph (Pearson and Zhang, 2014, 2015), which allows vertices to appear multiple times in one hyperedge. The embedding step is formulated in a regularization form with tensor decomposition, which represents each vertex as a low-dimensional numerical vector and encourages vertices within the same community to be close in the embedding space. The proposed hypergraph embedding model is flexible and general, which includes the hypergraph stochastic block model (hSBM), also known as hypergraph planted partition model (Ghoshdastidar and Dukkipati, 2017a), as its special case. It also accommodates heterogeneity among vertices by allowing vertices within a community to fluctuate in all directions. This is in sharp contrast to hSBM, which assumes vertices within a community share the same spectral embedding vector. It is also more general than the hypergraph degree-corrected block model (hDCBM; Ke et al. 2021; Yuan et al. 2021), un-

der which spectral embeddings of vertices within a community are along the same direction and only differ by their magnitudes. The advantage of the proposed method is supported in both asymptotic theories and numerical experiments on a number of synthetic and real hypergraph networks.

The main contribution of this paper is three-fold. First, we propose a novel hypergraph embedding model (HEM), which consists of an augmentation step and an embedding step. The augmentation step introduces only one null vertex rather than multiple ones as suggested in Ouvrard et al. (2021), which is more efficient and greatly facilitates the subsequent community detection. The embedding step, to the best of our knowledge, is the first statistical framework that extends the latent space model for graph network to general hypergraph network with theoretical guarantees. Second, a joint modeling framework is developed for simultaneously conducting hypergraph estimation and community detection. Third, we establish the asymptotic consistencies of the proposed method in terms of both hypergraph estimation and community detection in sparse hypergraph network. Particularly, the consistencies hold as long as the link probability is of the order  $s_n \gg n^{1-m} \log n$  in an  $m$ th-order hypergraph with  $n$  vertices. This result compares favorably with the existing sparsity results in literature (Ke et al., 2021; Ghoshdastidar and Dukkipati, 2017a,b), not to mention that the proposed method also achieves fast convergence rate in hypergraph estimation.

The rest of the paper is organized as follows. Section 2 provides a quick review of some preliminaries on hypergraph and tensor. Section 3 presents the details of the proposed hypergraph augmentation and embedding formulations, and an efficient optimization algorithm. Section 4 establishes the asymptotic consistencies of the proposed method. Section 5 examines the numerical performance of the proposed method on both synthetic and real-life hypergraph networks. Section 6 concludes the paper, and technical proofs and necessary lemmas are contained in the supplementary files.

## 2 Preliminaries

To begin with, we introduce some basic concepts of hypergraph and tensor that will be used extensively in the sequel. A general hypergraph is denoted as  $\mathcal{H}(V, E)$ , where  $V = \{v_1, v_2, \dots, v_n\}$  is a vertex set with  $n$  vertices,  $E$  consists of all hyperedges, and each hyperedge may contain multiple vertices in  $V$ . Denote  $[n] = \{1, 2, \dots, n\}$ , and we set  $V = [n]$  for simplicity, and thus a hyperedge is a non-empty subset of  $[n]$ . A hypergraph is called  $m$ -uniform if the cardinality of every hyperedge equals  $m$ . On the flip side, a non-uniform hypergraph contains hyperedges whose cardinalities can vary from one to another. A simple non-uniform hypergraph with 5 vertices and 5 hyperedges is displayed in the left panel of Figure 1, where hyperedges  $e_1$  and  $e_2$  consist of 3 vertices, hyperedges  $e_3$  and  $e_4$  consist of 2 vertices, and hyperedge  $e_5$  consists of 4 vertices. Note that the hypergraphs considered in this paper are undirected; that is, no ordering of vertices is necessary within the hyperedges. For definition of directed hypergraph, interested readers may refer to Gallo et al. (1993) and Ouvrard et al. (2021).

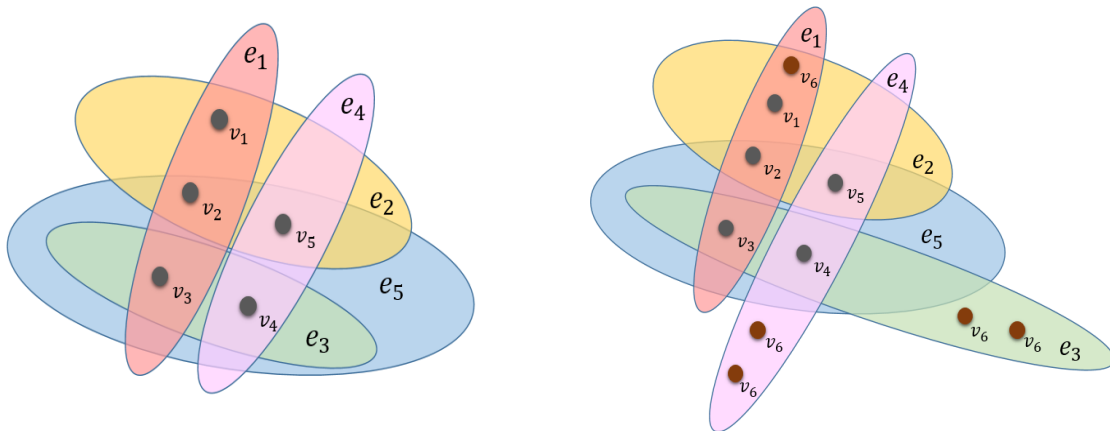


Figure 1: A non-uniform hypergraph with 5 vertices and 5 hyperedges (left) and the corresponding augmented 4-uniform multi-hypergraph (right).

A tensor  $\mathcal{A} = (a_{i_1 \dots i_m}) \in \mathbb{R}^{I_1 \times \dots \times I_m}$  is a cubical tensor if  $I_1 = \dots = I_m = n$ , for some  $n \in \mathbb{Z}^+$ . More formally, such a tensor is called an  $m$ th-order tensor of dimension  $n$ . A cubical

tensor  $\mathcal{A}$  is super symmetric if  $a_{i_1 \dots i_m} = a_{\pi(i_1) \dots \pi(i_m)}$ , for any possible permutations  $\pi \in S_m$ , the symmetric group of degree  $m$ . A  $m$ th-order super symmetric tensor  $\mathcal{I} \in \{0, 1\}^{n \times \dots \times n}$  is called an identity tensor if  $I_{i_1 \dots i_m} = 1$  when  $i_1 = \dots = i_m$  and 0 otherwise.

Let  $M^{(j)} \in \mathbb{R}^{Q_j \times I_j}$  be  $m$  matrices, then the mode  $j$  product (Kolda and Bader, 2009) between  $\mathcal{A}$  and  $M^{(j)}$  is defined as  $\mathcal{A} \times_j M^{(j)} \in \mathbb{R}^{I_1 \times \dots \times I_{j-1} \times Q_j \times I_{j+1} \times \dots \times I_m}$  with entries

$$(\mathcal{A} \times_j M^{(j)})_{i_1 \dots i_{j-1} q_j i_{j+1} \dots i_m} = \sum_{i_j=1}^{I_j} a_{i_1 \dots i_{j-1} i_j i_{j+1} \dots i_m} M_{q_j i_j}^{(j)}.$$

Moreover,  $\mathcal{A} \times_1 M^{(1)} \times_2 \dots \times_m M^{(m)} \in \mathbb{R}^{Q_1 \times \dots \times Q_m}$  is such a tensor with entries

$$(\mathcal{A} \times_1 M^{(1)} \times_2 \dots \times_m M^{(m)})_{q_1 \dots q_m} = \sum_{i_1=1}^{I_1} \dots \sum_{i_m=1}^{I_m} a_{i_1 \dots i_m} M_{q_1 i_1}^{(1)} \dots M_{q_m i_m}^{(m)}.$$

Recall that a multi-set  $\{\{i_1, i_2, \dots, i_m\}\}$  is an extension of set in that some elements may appear multiple times. Herein, to distinguish from a set, we use double curly braces  $\{\{\cdot\}\}$  to denote a multi-set as in Bahmanian and Sajna (2015) and Kovačević and Tan (2018). Clearly, if the elements  $i_1, \dots, i_m$  are distinct with one another, the multi-set  $\{\{i_1, \dots, i_m\}\}$  reduces to the set  $\{i_1, \dots, i_m\}$ . For any  $i_1, \dots, i_m \in [n+1]$ , we define an augmented Kronecker delta to be  $\delta_{i_1 \dots i_m}^{n+1} = 0$  if  $\{\{i_1, \dots, i_m\}\} \setminus \{n+1\}$  is indeed a non-empty set and 1 otherwise, where the multi-set difference with a set  $\{\{i_1, \dots, i_m\}\} \setminus \{n+1\}$  is a multi-set containing elements in the multi-set  $\{\{i_1, \dots, i_m\}\}$  but not in the set  $\{n+1\}$ . For example, if  $n = 100$  and  $m = 3$ , we have  $\delta_{1,2,101}^{101} = 0$ ,  $\delta_{101,101,101}^{101} = 1$  and  $\delta_{1,1,2}^{101} = 1$ . Furthermore, the order-specified augmented Kronecker delta  $\delta_{i_1 \dots i_m}^{n+1, ord} = 0$  if and only if  $\delta_{i_1 \dots i_m}^{n+1} = 0$  and  $i_1 \leq \dots \leq i_m$ . These two extended Kronecker deltas can greatly simplify notations and formulations for non-uniform hypergraph, and they are slightly different from the vanilla extension in Qi (2005), where the extended Kronecker delta equals 0 if there exist at least 2 distinct elements.

### 3 Community detection in hypergraph

This section proposes a novel community detection method for general hypergraphs. The key idea is to introduce a null vertex so that hyperedges with smaller cardinality can be augmented, and the non-uniform hypergraph is transformed into a special uniform multi-hypergraph, where the null vertex may appear multiple times in some hyperedges. Then the proposed method proceeds to seek for a suitable numeric embedding that embeds all vertices of the hypergraph into a low dimensional Euclidean space, where vertices belong to the same community tend to have shorter distance.

#### 3.1 Hypergraph augmentation

Let  $\mathcal{H}(V, E)$  be a hypergraph, possibly non-uniform, with  $V = [n]$  and range  $m \geq 2$ , which is the maximum cardinality of a hyperedge in  $E$ . One of the key challenges of analyzing non-uniform hypergraph is due to the unequal hyperedge cardinalities, leading to the ambiguity of discriminating hyperedges and their proper subsets.

To circumvent this difficulty, we introduce a null vertex, denoted as  $v_{n+1}$ , and then any hyperedge with cardinality less than  $m$  can be augmented to a multi-set with  $m$  elements. For instance, when  $m > 3$ , a hyperedge with vertices  $\{1, 2, 3\}$  can be augmented to  $\{\{1, 2, 3, n + 1, \dots, n + 1\}\}$  with  $m - 3$  null vertices, whereas another hyperedge with vertices  $\{1, \dots, m\}$  stays the same without any additional null vertex. It is clear that  $\mathcal{H}$  is converted to an equivalent  $m$ -uniform multi-hypergraph, where each hyperedge is a multi-set with cardinality  $m$  and only the null vertex  $v_{n+1}$  is allowed to appear multiple times in a hyperedge. With slight abuse of notation, we still denote this  $m$ -uniform multi-hypergraph as  $\mathcal{H}$ . A simple illustration of this augmentation step is displayed in the right panel of Figure 1.

We remark that when  $\mathcal{H}$  is a uniform hypergraph, the augmentation step and the subsequent special treatments of the null vertex are not necessary. For ease of presentation, we

assume  $\mathcal{H}$  is a non-uniform hypergraph hereafter, and the upcoming proposed model can be adapted to uniform hypergraph with slight modification. As such, we use the  $m$ th-order adjacency tensor  $\mathcal{A} = (a_{i_1 \dots i_m}) \in \{0, 1\}^{(n+1) \times \dots \times (n+1)}$  to represent  $\mathcal{H}$  with entries

$$a_{i_1 \dots i_m} = \begin{cases} 1 & \text{if } \{\{i_1, \dots, i_m\} \setminus \{n+1\}\} \in E; \\ 0 & \text{otherwise.} \end{cases}$$

Apparently, a necessary condition for  $a_{i_1 \dots i_m} = 1$  is  $\delta_{i_1 \dots i_m}^{n+1} = 0$ . It is clear that this augmentation step, converting a non-uniform hypergraph to a uniform multi-hypergraph, is critical to make downstream analyses more statistically and computationally tractable.

Suppose there are  $K$  potential communities within the hypergraph, and let  $\psi : [n] \rightarrow [K]$  be the community assignment function, then  $\psi(i) = s$  if vertex  $v_i$  belongs to the  $s$ -th community. We also write  $\psi_i = \psi(i)$  for short. Note that the null vertex  $v_{n+1}$  does not belong to any community, and thus we set  $\psi_{n+1} = K + 1$  for formality. Denote  $Z = (z_{ij}) \in \mathbb{R}^{(n+1) \times (K+1)}$  to be the corresponding community membership matrix with  $z_{ij} = 1$  if  $j = \psi_i$  and 0 otherwise. It is obvious that  $z_{i, K+1} = 1$  only when  $i = n + 1$ .

### 3.2 Hypergraph embedding

Given the  $m$ -uniform multi-hypergraph  $\mathcal{H}$  from the augmentation step, we let  $\mathcal{P} = (p_{i_1 \dots i_m}) \in (0, 1)^{(n+1) \times \dots \times (n+1)}$  be the  $m$ th-order probability tensor, with  $p_{i_1 \dots i_m} = P(a_{i_1 \dots i_m} = 1)$  if  $\delta_{i_1 \dots i_m}^{n+1} = 0$ , and let  $\Theta = (\theta_{i_1 \dots i_m}) \in \mathbb{R}^{(n+1) \times \dots \times (n+1)}$  be the entrywise transformation of  $\mathcal{P}$  so that

$$\theta_{i_1 \dots i_m} = \log \left( \frac{p_{i_1 \dots i_m}}{s_n - p_{i_1 \dots i_m}} \right), \quad (1)$$

where the sparsity factor  $s_n$  that may vanish with  $n$  is introduced to accommodate sparse networks. The modified logit transformation (1) implies that  $p_{i_1 \dots i_m} = s_n(1 + e^{-\theta_{i_1 \dots i_m}})^{-1}$ , and



the number of hyperedges is of order  $O_p(s_n n^m)$  if  $\Theta$  lies in a compact subset of  $\mathbb{R}^{(n+1) \times \dots \times (n+1)}$ . We remark that many frequentist analysis of network models multiplies the network underlying linking probability by a decaying sparsity coefficient to accommodate sparse networks, such as the hypergraph stochastic block model (Ghoshdastidar and Dukkipati, 2017a,b) and hypergraph degree-corrected block model (Ke et al., 2021). Yet this treatment may not be directly applied to latent space model with standard logit transformation, since tiny value of  $p_{i_1 \dots i_m}$  implies that  $\theta_{i_1 \dots i_m}$  will be pushed towards  $-\infty$ , and thus the entries of  $\alpha$  may diverge to  $\pm\infty$ , leading to unstable numerical performance in estimating  $\alpha$ .

We now turn to embed the hypergraph into an  $r$ -dimensional Euclidean space with  $2 \leq r \ll n$ , where each vertex is represented by an  $r$ -dimensional vector  $\alpha_i$  for any  $i \in [n]$ . The embedding dimension  $r$  here is allowed to diverge with  $n$ . For the null vertex, we simply set  $\alpha_{n+1} = r^{-1/2} \mathbf{1}_r$ , the  $r$  dimensional vector with every entry  $r^{-1/2}$ . Let  $\alpha = (\alpha_1, \dots, \alpha_{n+1})^T$  be the embedding matrix. We consider the following hypergraph embedding model (HEM),

$$\Theta = \mathcal{I} \times_1 \alpha \times_2 \dots \times_m \alpha, \quad (2)$$

where  $\mathcal{I} \in \mathbb{R}^{r \times \dots \times r}$  is the  $m$ th-order identity tensor of dimension  $r$ . Clearly, for any  $i_1, \dots, i_m \in [n+1]$ , model (2) assumes that the information contained in  $\theta_{i_1 \dots i_m}$  can be fully captured by the embedding matrix  $\alpha$  in that  $\theta_{i_1 \dots i_m} = \mathcal{I} \times_1 \alpha_{i_1}^T \times_2 \dots \times_m \alpha_{i_m}^T$ . When  $\delta_{i_1 \dots i_m}^{n+1, ord} = 0$ , the probability that  $\{\{i_1, \dots, i_m\}\} \setminus \{n+1\}$  forms a hyperedge is  $s_n(1 + e^{-\theta_{i_1 \dots i_m}})^{-1}$ , whereas  $\theta_{i_1 \dots i_m}$  or  $p_{i_1 \dots i_m}$  defined in (2) does not have any probability interpretation when  $\delta_{i_1 \dots i_m}^{n+1, ord} = 1$ , and is thus inconsequential.

The proposed HEM is flexible and general, and includes the celebrated hSBM (Ghoshdastidar and Dukkipati, 2017a) as its special case. Particularly, taking  $\alpha = ZC$ , HEM reduces to  $\Theta = \mathcal{B} \times_1 Z \times_2 \dots \times_m Z$  with  $\mathcal{B} = \mathcal{I} \times_1 C \times_2 \dots \times_m C$ , which becomes an hSBM with membership matrix  $Z \in \{0, 1\}^{(n+1) \times (K+1)}$  and a transformed core probability tensor

$\mathcal{B} \in \mathbb{R}^{(K+1) \times \dots \times (K+1)}$ . Yet, HEM is more flexible as it naturally accommodates heterogeneity among vertices by allowing the embeddings or spectral embeddings of vertex within a community to fluctuate in all directions. It is worth pointing out that such accommodation of heterogeneity is more general than that in hDCBM (Ke et al., 2021; Yuan et al., 2021), which requires spectral embeddings of vertices within a community to lie along the same direction and only differ by magnitudes.

It is also interesting to remark that HEM is equivalent to assuming that the super symmetry tensor  $\Theta$  has a symmetric CP decomposition (Kolda and Bader, 2009),  $\Theta = \sum_{j=1}^r \alpha_{.j} \circ \dots \circ \alpha_{.j}$ , where  $\alpha_{.j}$  is the  $j$ -th column of  $\alpha$  and  $\circ$  stands for the vector outer product. Furthermore, we define the symmetric rank of an  $m$ th-order tensor  $\Theta$  of dimension  $n + 1$  over  $\mathbb{R}$  as  $\text{rank}(\Theta) = \min\{R : \Theta = \sum_{r=1}^R u_r \circ \dots \circ u_r, u_r \in \mathbb{R}^{n+1}\}$ . Therefore, it is assumed that  $\Theta$  has symmetric rank at most  $r$ . We also remark our definition of symmetric rank is slightly different from the one that defined in literature (Kolda and Bader, 2009; Robeva, 2016) by requiring the embedding vectors to be real.

More importantly, HEM is identifiable if  $\Theta$  has symmetric rank  $r$  and  $m \geq 3$ , as the factorization (2) is unique up to column permutations of  $\alpha$  (Sidiropoulos and Bro, 2000). When  $\Theta$  has symmetric rank  $r$  but  $m = 2$ , HEM reduces to the latent space model for graph networks (Hoff et al., 2002) and the factorization (2) is unique up to any orthogonal transformation of  $\alpha$ . Note that column permutations or general orthogonal transformations are isometric linear transformation of the rows of  $\alpha$ , the community structure encoded in  $\alpha$  always remains unchanged.

### 3.3 Penalized log-likelihood objective

With the factorization of  $\Theta$  in (2), the negative log-likelihood function of  $\mathcal{H}$  becomes

$$\mathcal{L}(\boldsymbol{\alpha}; \mathcal{A}) = \frac{1}{\varphi(n, m)} \sum_{\delta_{i_1 \dots i_m}^{n+1, ord} = 0} L(\theta_{i_1 \dots i_m}; a_{i_1 \dots i_m}),$$

where  $\varphi(n, m) = \sum_{k=1}^m \binom{n}{k}$  is the number of potential hyperedges with  $\delta_{i_1 \dots i_m}^{n+1, ord} = 0$ ,  $\theta_{i_1 \dots i_m} = \mathcal{I} \times_1 \boldsymbol{\alpha}_{i_1}^T \times_2 \dots \times_m \boldsymbol{\alpha}_{i_m}^T$ , and

$$L(\theta_{i_1 \dots i_m}; a_{i_1 \dots i_m}) = \log \left( 1 + \frac{s_n}{1 - s_n + e^{-\theta_{i_1 \dots i_m}}} \right) - a_{i_1 \dots i_m} \log \left( \frac{s_n}{1 - s_n + e^{-\theta_{i_1 \dots i_m}}} \right).$$

We next equip  $\mathcal{L}(\boldsymbol{\alpha}; \mathcal{A})$  with a novel penalty term to enhance the feasibility of computation and hypergraph community detection. This leads to the proposed regularized cost function,

$$\mathcal{L}_\lambda(\boldsymbol{\alpha}; \mathcal{A}) = \mathcal{L}(\boldsymbol{\alpha}; \mathcal{A}) + \lambda_n J(\boldsymbol{\alpha}), \quad (3)$$

where  $\lambda_n$  is a positive tuning parameter and

$$J(\boldsymbol{\alpha}) = \min_{Z \in \Gamma, C \in \mathcal{R}^{(K+1) \times r}} \frac{1}{n} \|\boldsymbol{\alpha} - ZC\|_F^2, \quad C_{K+1} = r^{-1/2} \mathbf{1}_r, \quad (4)$$

is introduced to encourage the community structure encoded in  $\boldsymbol{\alpha}$ . Herein,  $\Gamma$  is the set of all possible community membership matrix. That is, for any  $Z \in \Gamma \subset \mathbb{R}^{(n+1) \times (K+1)}$ , each row of  $Z$  contains exactly one 1 with all other entries being zeros, and  $Z_{i(K+1)} = 1$  if and only if  $i = n + 1$ . It is clear that the embeddings of vertices with similar linking patterns will be pushed towards the same center, and thus close to each other in the embedding space, leading to the desired community structure in  $\mathcal{H}$ . A similar regularization term has been employed in Tang et al. (2020) for individualized variable selection and in Zhang et al. (2021)

for community detection in directed networks. In the sequel, with  $\Theta = \mathcal{I} \times_1 \boldsymbol{\alpha} \dots \times_m \boldsymbol{\alpha}$ , we use  $\mathcal{L}_\lambda(\Theta; \mathcal{A})$  and  $\mathcal{L}_\lambda(\boldsymbol{\alpha}; \mathcal{A})$  interchangeably, as convenience dictates.

We develop an alternative updating scheme to minimize (3). Particularly, given  $Z^{(t)}$  and  $C^{(t)}$  at step  $t$ ,  $\boldsymbol{\alpha}$  can be updated by solving

$$\min_{\boldsymbol{\alpha}_{n+1}=r^{-1/2}\mathbf{1}_r} \frac{1}{\varphi(n, m)} \sum_{\delta_{i_1 \dots i_m}^{n+1, ord}=0} L(\theta_{i_1 \dots i_m}; a_{i_1 \dots i_m}) + \frac{\lambda_n}{n} \|\boldsymbol{\alpha} - Z^{(t)}C^{(t)}\|_F^2.$$

Denote  $\mathcal{T} = \frac{\partial \mathcal{L}(\Theta, \mathcal{A})}{\partial \Theta}$ , and let  $\Delta = \{0, 1\}^{(n+1) \times \dots \times (n+1)}$  such that  $\Delta_{i_1, \dots, i_m} = 1$  if  $\delta_{i_1 i_2 \dots i_m}^{n+1} = 0$  with  $\delta_{i_2 i_3 \dots i_m}^{n+1, ord} = 0$  or  $\delta_{i_1 (n+1) \dots (n+1)}^{n+1} = 0$ , and 0 otherwise. We then update the first  $n$  rows of  $\boldsymbol{\alpha}$ , which is denoted as  $\boldsymbol{\alpha}_{1:n}$ , along its gradient,  $\boldsymbol{\alpha}_{1:n}^{(t+1)} = \boldsymbol{\alpha}_{1:n}^{(t)} - \eta_t \nabla_{\boldsymbol{\alpha}_{1:n}} \mathcal{L}_\lambda^{(t)}(\boldsymbol{\alpha}^{(t)})$ , where  $\eta_t > 0$  is the learning rate at step  $t + 1$ , and

$$\nabla_{\boldsymbol{\alpha}_{1:n}} \mathcal{L}_\lambda^{(t)}(\boldsymbol{\alpha}^{(t)}) = \frac{1}{\varphi(n, m)} \langle \mathcal{T} * \Delta, \mathcal{I} \times_2 \boldsymbol{\alpha} \times_3 \dots \times_m \boldsymbol{\alpha} \rangle_{1:n}^{\{2, \dots, m\}} + \frac{2\lambda_n}{n} (\boldsymbol{\alpha} - Z^{(t)}C^{(t)})_{1:n}.$$

Herein,  $*$  is the Hadamard product (entry-wise product) between two tensors, and  $\langle \mathcal{T} * \Delta, \mathcal{I} \times_2 \boldsymbol{\alpha} \times_3 \dots \times_m \boldsymbol{\alpha} \rangle_{1:n}^{\{2, \dots, m\}} \in \mathbb{R}^{(n+1) \times r}$  is the tensor inner product between  $\mathcal{T} * \Delta$  and  $\mathcal{I} \times_2 \boldsymbol{\alpha} \times_3 \dots \times_m \boldsymbol{\alpha}$  with respect to the second, ...,  $m$ -th modes. Specifically, the  $(i, j)$ -th entry of  $\langle \mathcal{T} * \Delta, \mathcal{I} \times_2 \boldsymbol{\alpha} \times_3 \dots \times_m \boldsymbol{\alpha} \rangle_{1:n}^{\{2, \dots, m\}}$  is  $\sum_{i_2, \dots, i_m} (\mathcal{T} * \Delta)_{ii_2 \dots i_m} (\mathcal{I} \times_2 \boldsymbol{\alpha} \times_3 \dots \times_m \boldsymbol{\alpha})_{ji_2 \dots i_m}$ .

Next, given  $\boldsymbol{\alpha}^{(t+1)}$ , the sub-optimization task now becomes

$$\min_{Z \in \Gamma, C \in \mathcal{R}^{(K+1) \times r}} \frac{1}{n} \|\boldsymbol{\alpha}^{(t+1)} - ZC\|_F^2, \text{ subject to } C_{K+1} = r^{-1/2}\mathbf{1}_r. \quad (5)$$

Clearly, it resembles the K-means formulation for  $\boldsymbol{\alpha}_{1:n}^{(t+1)}$ , and thus a standard K-means algorithm can be employed to solve for  $Z$  and  $C$ .

As computational remarks, the alternative updating algorithm is guaranteed to converge to a stationary point, and its computational complexity is of order  $O(\kappa_2(n^m r + \kappa_1 K n r))$ ,

where  $\kappa_1$  is the number of iterations for the  $K$ -means algorithm and  $\kappa_2$  is the number of iterations for the gradient descent step. Note that low rank tensor approximation tends to be computationally expensive and easy to get trapped in non-informative local minima (Arous et al., 2019). Based on our limited numerical experience, a warm initialization of  $\boldsymbol{\alpha}^{(0)}$  can greatly help with the numerical convergence. In all the numerical examples, we initialize  $\boldsymbol{\alpha}^{(0)}$  with a higher-order singular value decomposition algorithm (HOSVD; De Lathauwer et al., 2000). We also suggest to set the embedding dimension  $r = K$  in practice, similar suggestions were also made for some spectral-clustering-based algorithms (Ghoshdastidar and Dukkipati, 2017a). When  $K$  is unknown, we can follow the procedure in Ke et al. (2021) to investigate the “eigen-gap” of the network adjacency tensor. Specifically, one can first obtain a spectral embedding  $\widehat{U}$  with sufficiently large dimension, and then investigate the eigen-gap of the matrix  $\mathcal{M}_1(\mathcal{A} \times_3 \widehat{U} \times_4 \dots \times_m \widehat{U})$ . Other data adaptive selection criteria, such as network cross-validation (Chen and Lei, 2018; Li et al., 2020a) may be employed as well, at the cost of increased computational burden.

## 4 Asymptotic theory

This section establishes some theoretic results to quantify the asymptotic behavior of the proposed HEM method in estimating the underlying transformed probability tensor  $\Theta$  as well as detecting community structure in a general hypergraph.

### 4.1 Consistency in estimating $\Theta^*$

Let  $\Omega = \{\Theta : \Theta = \mathcal{I} \times_1 \boldsymbol{\alpha} \times_2 \dots \times_m \boldsymbol{\alpha}, \max_{i \in [n+1]} \|\boldsymbol{\alpha}_i\|_2 \leq c_0, \boldsymbol{\alpha}_{n+1} = r^{-1/2} \mathbf{1}_r\} \subset \mathbb{R}^{(n+1) \times \dots \times (n+1)}$  be the domain of the problem, for a positive constant  $c_0 \geq 1$ . It is clear that  $\Omega$  is a compact subset of  $\mathbb{R}^{(n+1) \times \dots \times (n+1)}$ , and for any  $\Theta \in \Omega$ , it has symmetric rank at most  $r$ . Denote  $\boldsymbol{\alpha}^*$  as the underlying true hypergraph embedding with  $\Theta^* = \mathcal{I} \times_1 \boldsymbol{\alpha}^* \times_2 \dots \times_m \boldsymbol{\alpha}^* \in \Omega$ . In

addition, for any  $\Theta \in \Omega$ , we define  $e_L(\Theta, \Theta^*) = \varphi^{-1}(n, m) \sum_{\delta_{i_1 \dots i_m}^{n+1, ord=0}} E(L(\theta_{i_1 \dots i_m}; a_{i_1 \dots i_m}) - L(\theta_{i_1 \dots i_m}^*; a_{i_1 \dots i_m}))$ , which is the average of certain Kullback-Leibler divergences and guaranteed to be non-negative.

The following large deviation inequality is derived to quantify the asymptotic behavior of  $\mathcal{L}_\lambda(\Theta; \mathcal{A})$  in the neighborhood of  $\Theta^*$  defined by  $e_L(\Theta, \Theta^*)$ .

**Proposition 1.** *Suppose  $\lambda_n J(\boldsymbol{\alpha}^*) < \frac{1}{2}\epsilon_n$ , then there exists some absolute constants  $c_1, c_2$  such that if  $nr\varphi^{-1}(n, m)\epsilon_n^{-1} \log \epsilon_n^{-1/2} \leq c_1$ , we have*

$$P\left(\sup_{\{\Theta \in \Omega | e_L(\Theta, \Theta^*) \geq \epsilon_n\}} (\mathcal{L}_\lambda(\Theta^*; \mathcal{A}) - \mathcal{L}_\lambda(\Theta; \mathcal{A})) \geq 0\right) \leq 2 \exp(-c_2 \varphi(n, m) \epsilon_n).$$

Proposition 1 gives an intermediate result for establishing estimation consistency in Theorem 1, and it assures that any  $\Theta$  such that  $\mathcal{L}_\lambda(\Theta; \mathcal{A}) \leq \mathcal{L}_\lambda(\Theta^*; \mathcal{A})$  shall lie in the neighborhood of  $\Theta^*$  with high probability. By the condition that  $nr\varphi^{-1}(n, m)\epsilon_n^{-1} \log \epsilon_n^{-1/2} \leq c_1$ , the fastest order of  $\epsilon_n$  can be set as  $\epsilon_n = \frac{nr \log n}{\varphi(n, m)}$ , which is governed by the network size  $\varphi(n, m)$  and the number of parameters  $nr$  in HEM. It is interesting to remark that  $\lambda_n$  appears to have no effect on the order of  $\epsilon_n$ , as long as it satisfies the condition  $\lambda_n J(\boldsymbol{\alpha}^*) \leq \frac{1}{2}\epsilon_n$ .

We are now ready to establish the consistency of  $\widehat{\Theta} = \mathcal{I} \times_1 \widehat{\boldsymbol{\alpha}} \times_2 \dots \times_m \widehat{\boldsymbol{\alpha}}$ , with  $\widehat{\boldsymbol{\alpha}}$  being the estimate from Section 3.3. Let  $p(y; \theta)$  be the density of a Bernoulli random variable with parameter  $p = s_n(1 + \exp(-\theta))^{-1}$ . Then the discrete Hellinger distance between  $p(y; \theta)$  and  $p(y; \theta^*)$  is defined as

$$d(\theta, \theta^*) = \left[ (p^{1/2} - (p^*)^{1/2})^2 + ((1-p)^{1/2} - (1-p^*)^{1/2})^2 \right]^{1/2},$$

and the deviation between  $\Theta$  from  $\Theta^*$  can be evaluated by the averaged squared Hellinger distance,

$$D^2(\Theta, \Theta^*) = \frac{1}{\varphi(n, m)} \sum_{\delta_{i_1 \dots i_m}^{n+1, ord=0}} d^2(\theta_{i_1 \dots i_m}, \theta_{i_1 \dots i_m}^*).$$

**Theorem 1.** *Under the assumptions in Proposition 1, for any  $\widehat{\Theta}$  with  $\mathcal{L}_\lambda(\widehat{\alpha}; \mathcal{A}) \leq \mathcal{L}_\lambda(\alpha^*; \mathcal{A})$ , we have*

$$P(D^2(\widehat{\Theta}, \Theta^*) \geq \epsilon_n) \leq 2 \exp(-c_2 \varphi(n, m) \epsilon_n),$$

Moreover,  $D^2(\widehat{\Theta}, \Theta^*) = O_p(\epsilon_n)$  and  $n^{-m/2} \|\widehat{\Theta} - \Theta^*\|_F = O_p(\sqrt{\epsilon_n/s_n})$ .

Theorem 1 shows that a reasonably good solution  $\widehat{\Theta}$  is guaranteed to converge to  $\Theta^*$  at a fast rate, which depends on the centrality of the community structure encoded in  $\alpha^*$ , the network size and number of parameters via  $\epsilon_n$ , and the network sparsity factor  $s_n$ . The condition  $\mathcal{L}_\lambda(\widehat{\alpha}; \mathcal{A}) \leq \mathcal{L}_\lambda(\alpha^*; \mathcal{A})$  shall be satisfied by the solution obtained in Section 3.3, when the estimation algorithm is initialized by some value in a small neighborhood of  $\Theta^*$ . The consistency result in Theorem 1 holds true with  $O(rn^{1-m} \log n) \leq \epsilon_n \ll s_n$ . If we further set  $r < \log n$ , this yields a slightly weaker sparsity assumption than that in Ke et al. (2021) and Ghoshdastidar and Dukkipati (2017a,b), where the smallest sparsity factor is of the order  $n^{1-m}(\log n)^2$  for some fixed  $K$ .

## 4.2 Consistency in community detection

We now turn to establish the consistency of community detection for general hypergraphs. Let  $\psi^* : [n] \rightarrow [K]$  be the true community assignment function, and  $\widehat{\psi}$  be the estimation counterpart induced by  $\widehat{\alpha}$ . Formally,  $\widehat{\psi}_i = \arg \min_{k \in [K]} \|\alpha_i - \widehat{C}_k\|_2$ , where  $\widehat{C} = \arg \min_C \min_{Z \in \Gamma} \|\widehat{\alpha} - ZC\|_F$ , subject to  $C_{K+1} = r^{-1/2} \mathbf{1}_r$ . The community detection error of  $\widehat{\psi}$  can be evaluated by the minimum scaled Hamming distance between  $\widehat{\psi}$  and  $\psi^*$  under permutations, which is defined as

$$\text{err}(\psi^*, \widehat{\psi}) = \min_{\pi \in S_K} \frac{1}{n} \sum_{i=1}^n \mathbf{1}\{\psi_i^* \neq \pi(\widehat{\psi}_i)\}, \quad (6)$$

where  $\mathbf{1}\{\cdot\}$  is the indicator function and  $S_K$  is the symmetric group of degree  $K$ . Clearly, it measures the minimum fraction of vertices that are misclassified by  $\hat{\psi}$  under permutation, and  $\hat{\psi}$  is a consistent estimator of  $\psi^*$  if  $\text{err}(\psi^*, \hat{\psi})$  goes to zero with probability tending to 1. Such a scaled or unscaled Hamming distance has become a popular metric in quantifying the performance of community detection (Ghoshdastidar and Dukkipati, 2017b,a; Ke et al., 2021; Jing et al., 2021; Lee et al., 2021).

Let  $N_k^* = \{i : \psi_i^* = k\}$  be a true network community with cardinality  $n_k$  and  $C^* \in \mathbb{R}^{(K+1) \times r}$  be the associated community embedding center matrix in the sense that  $C_k^* = \frac{1}{n_k} \sum_{\psi_i^*=k} \alpha_i^*$ , for  $k \in [K]$ , and  $C_{K+1}^* = r^{-1/2} \mathbf{1}_r$ . Denote  $\mathcal{B}^* = \mathcal{I} \times_1 C^* \times_2 \dots \times_m C^*$ . The following assumptions are made to ensure that communities within the hypergraph networks are asymptotically identifiable.

**Assumption A.** *There exists a constant  $c_3 > 0$  such that*

$$\min_{k, k' \in [K], k \neq k'} K^{(1-m)/2} \|\mathcal{B}_k^* - \mathcal{B}_{k'}^*\|_F \geq c_3 \gamma_n,$$

where  $\mathcal{B}_k^*$  is the  $k$ -th sub-tensor of  $\mathcal{B}^*$  by fixing the first index as  $k$ , and  $\gamma_n$  may converge to 0 with  $n$ .

**Assumption B.** *There exists a constant  $c_4$  such that  $\max_k n_k \leq c_4 \min_k n_k$ .*

Assumption A is an identifiability assumption, which assumes that the true communities are well separated as  $n$  grows, and is crucial to the feasibility of community detection. It is interesting to remark that a signal-to-noise ratio is used in Yuan et al. (2021) to characterizes the separability among communities under hSBM. A similar community separation assumption can be found in Lei et al. (2019) for multi-layer network model. Assumption B assures the communities are well defined and will not degenerate asymptotically. This assumption is mild and satisfied when the vertex community memberships come from a multinomial dis-



tribution. The same assumption can be found in Ke et al. (2021), and a relatively stronger assumption can be found in Chien et al. (2019) assuming equal community sizes.

**Theorem 2.** *Suppose all the assumptions in Theorem 1 as well as Assumptions A and B are satisfied,  $\lim_{n \rightarrow +\infty} \lambda_n \epsilon_n s_n^{-2} (\log s_n^{-1})^{-1} > 0$  and  $K = o(\gamma_n^2 s_n \epsilon_n^{-1})$ , then  $\text{err}(\psi^*, \hat{\psi}) = O_p(\epsilon_n s_n^{-1} \gamma_n^{-2})$ .*

Theorem 2 assures that the community structure in a general hypergraph can be consistently recovered by the proposed HEM method. The consistency result holds true for diverging  $K$  as long as it does not diverge too fast. Furthermore, Theorem 2 requires that  $\lambda_n$  cannot be too small, whereas Theorem 1 requires  $\lambda_n$  to be sufficiently small. Combining these two gives a proper interval for the order of  $\lambda_n$  to assure consistency in both network estimation and community detection.

As a theoretical example, consider a hypergraph network with  $J(\boldsymbol{\alpha}^*) \leq \epsilon_n^2 (s_n^2 \log(s_n^{-1}))^{-1}$  and  $r$ ,  $\gamma_n$  and  $K$  are of the constant order. With  $\lambda_n = \frac{1}{2} \epsilon_n^{-1} s_n^2 \log(s_n^{-1})$ , Theorem 1 implies that  $\epsilon_n$  is of the order  $n^{1-m} \log n$ , and Theorem 2 further implies that  $\text{err}(\psi^*, \hat{\psi}) = O_p(\log n / (n^{m-1} s_n))$ , which matches up with the error rates in Ghoshdastidar and Dukkipati (2017a,b) and Ke et al. (2021). To ensure the community detection consistency, Theorem 2 requires that  $s_n \gg \log n / n^{m-1}$ , which is slightly weaker than the sparsity requirement in Ghoshdastidar and Dukkipati (2017a,b) and Ke et al. (2021). We also remark that under homogeneous hSBM, where the probability of any  $m$  vertices forming a hypergraph is  $p$  if they are from the same community and  $q$  otherwise, both error rates and sparsity requirement may be improved (Ahn et al., 2018). However, such results highly rely on the restrictive homogeneous hSBM, and it remains unclear whether they can be extended to heterogeneous hSBM or the even more general HEM.

## 5 Numerical experiments

We evaluate the performance of the proposed HEM method on a variety of synthetic and real-life non-uniform hypergraph network data. We compare its performance with some existing non-uniform hypergraph community detection methods in literature, including Tensor-SCORE (Ke et al., 2021), spectral hypergraph partitioning (SHP; Ghoshdastidar and Dukkipati (2017a)), and weighted projection to graph method (WPTG; Kumar et al. (2021); Ghoshdastidar and Dukkipati (2015a)). Tensor-SCORE is designed for uniform hypergraph community detection and can be extended to non-uniform hypergraph by representing non-uniform hypergraph as a collection of uniform hypergraphs or by adding multiple null vertices to convert the non-uniform hypergraph to a uniform one as in Ouvrard et al. (2021). We abbreviate the former extension as TS-1, while the latter extension as TS-2. SHP converts a non-uniform hypergraph to an incident matrix, and then maximizes the hypergraph associativity or minimizes the normalized hypergraph cut. WPTG represents the non-uniform hypergraph by a weighted adjacency matrix, and then standard graph community detection methods such as the spectral clustering, SCORE (Jin, 2015) and modularity maximization algorithms can be employed.

Both HEM and Tensor-SCORE involve some tuning parameters, which can be optimally determined by some data-adaptive selection criteria, including the stability criteria (Wang, 2010) or the network cross validation (Li et al., 2020a). Yet such data-adaptive selection schemes can be computationally expensive. Alternatively, in our numerical experiments, we follow the treatment in Ke et al. (2021) for the tuning parameters in Tensor-SCORE, and set  $\lambda_n = 10^{-4}/n$  for HEM to prevent  $J(\boldsymbol{\alpha})$  from vanishing too fast. We scale  $\lambda_n$  properly in order to ensure more information can be learned from the network likelihood at the early iterations in the computing algorithm. The numerical performance of all the methods is assessed by the average scaled Hamming error in (6).

## 5.1 Synthetic networks

We consider two scenarios of synthetic networks for numerical comparison.

**Scenario 1:** The non-uniform hypergraph networks are generated from the HEM model in (1) and (2). We vary the number of vertices  $n \in \{300, 400, 500\}$ , the sparsity factor  $s_n \in \{0.4, 0.2, 0.1, 0.05, 0.025\}$ , and set the range of all the hypergraphs to be  $m = 3$  with  $r = K = 2$ . First, we generate the community centers  $C^* \in \mathbb{R}^{(K+1) \times r}$  with  $C_k^* \sim N_r(\mathbf{0}_r, I_r)$  for  $k \in [K]$  and the last row  $C_{K+1} = r^{-1/2} \mathbf{1}_r$ , where  $I_r$  is the  $r$ -dimensional identity matrix. Next, the vertex community memberships  $\psi_i^*$ ,  $i \in [n]$ , are generated from the multinomial distribution with parameters  $\frac{1}{K} \mathbf{1}_K$  indicating that the communities are approximately of equal sizes. The community membership matrix  $Z^* \in \{0, 1\}^{(n+1) \times (K+1)}$  can be constructed accordingly. After that, the hypergraph embedding matrix is generated as  $\boldsymbol{\alpha}^* = Z^* C^* + \boldsymbol{\varepsilon}$ . Herein,  $\boldsymbol{\varepsilon}$  is a noise matrix with  $\varepsilon_{ij} \stackrel{i.i.d.}{\sim} N(0, 0.5^2)$  if  $i \in [n]$  and  $\varepsilon_{ij} = 0$  if  $i = n + 1$ . Finally,  $\mathcal{P}^*$  can be computed based on  $\boldsymbol{\alpha}^*$ . For  $i_1, i_2, i_3$  such that  $\delta_{i_1 i_2 i_3}^{n+1, ord} = 0$ , the hyperedge among vertices  $\{\{i_1, i_2, i_3\}\} \setminus \{n + 1\}$  is generated with probability  $p_{i_1 i_2 i_3}^*$  independently.

**Scenario 2:** The hypergraph generation process is the same as in Scenario 1, except that community sizes can be unbalanced. Specifically, we fix  $n = 300$ ,  $m = 3$ ,  $s_n = 0.1$  and  $r = K = 2$ , and vary the parameters of the multinomial distribution  $(\kappa_1, \kappa_2)$  such that  $\kappa_1 + \kappa_2 = 1$  and  $\kappa_1/\kappa_2 \in \{0.1, 0.3, 0.5, 0.7, 0.9\}$ . Clearly, as  $\kappa_1/\kappa_2$  gets smaller, the communities become more unbalanced.

For both scenarios, the averaged scaled Hamming errors and their corresponding standard errors of various community detection methods over 50 independent replications are reported in Tables 1 and 2.

It is evident that HEM yields the smallest community detection error among all the methods in both scenarios. The performance of HEM and Tensor-SCORE is much better than that of SHP and WPTG, mainly due to the fact that SHP and WPTG need to convert the hypergraph adjacency tensor to matrix and thus suffer from information loss. Further,

Table 1: The averaged community detection errors and its standard errors over 50 independent replications of different methods on the non-uniform hypergraph networks generated from Scenario 1.

$n$	$s_n$	HEM	TS-1	TS-2	SHP	WPTG
300	0.4	<b>0.1052</b> (0.0152)	0.1623(0.0200)	0.1556(0.0170)	0.2781(0.0270)	0.2901(0.0200)
	0.2	<b>0.0968</b> (0.0134)	0.1788(0.0206)	0.1561(0.0172)	0.2823(0.0210)	0.2874(0.0202)
	0.1	<b>0.1026</b> (0.0149)	0.1777(0.0197)	0.1587(0.0172)	0.2855(0.0206)	0.2925(0.0200)
	0.05	<b>0.1161</b> (0.0173)	0.1891(0.0216)	0.1627(0.0184)	0.2906(0.0202)	0.2969(0.0192)
	0.025	<b>0.1505</b> (0.0229)	0.1797(0.0208)	0.1659(0.0189)	0.3018(0.0199)	0.3077(0.0197)
400	0.4	<b>0.1094</b> (0.0159)	0.1592(0.0200)	0.1556(0.0167)	0.2814(0.0204)	0.2968(0.0197)
	0.2	<b>0.1003</b> (0.0145)	0.1780(0.0209)	0.1566(0.0168)	0.2825(0.0204)	0.2976(0.0197)
	0.1	<b>0.1120</b> (0.0155)	0.1811(0.0196)	0.1557(0.0167)	0.2868(0.0201)	0.2987(0.0194)
	0.05	<b>0.1251</b> (0.0184)	0.1802(0.0200)	0.1615(0.0175)	0.2918(0.0206)	0.2996(0.0198)
	0.025	<b>0.1342</b> (0.0213)	0.1874(0.0215)	0.1736(0.0197)	0.2964(0.0201)	0.3051(0.0196)
500	0.4	<b>0.1038</b> (0.0142)	0.1407(0.0173)	0.1483(0.0155)	0.2768(0.0205)	0.2848(0.0198)
	0.2	<b>0.0927</b> (0.0125)	0.1632(0.0195)	0.1524(0.0163)	0.2783(0.0205)	0.2834(0.0197)
	0.1	<b>0.0998</b> (0.0138)	0.1688(0.0198)	0.1524(0.0162)	0.2827(0.0209)	0.2873(0.0203)
	0.05	<b>0.1112</b> (0.0153)	0.1649(0.0182)	0.1542(0.0167)	0.2848(0.0208)	0.2904(0.0203)
	0.025	<b>0.1216</b> (0.0185)	0.1683(0.0192)	0.1561(0.0176)	0.2916(0.0203)	0.2931(0.0198)

Table 2: The averaged community detection errors and their corresponding standard errors over 50 independent replications of different methods on the non-uniform hypergraph networks generated from Scenario 2.

$\kappa_1/\kappa_2$	HEM	TS-1	TS-2	SHP	WPTG
0.1	0.2364(0.0233)	0.3930(0.0179)	<b>0.2236</b> (0.0246)	0.3467(0.0184)	0.3050(0.0225)
0.3	<b>0.1169</b> (0.0166)	0.2091(0.0259)	0.1639(0.0216)	0.3207(0.0211)	0.3066(0.0218)
0.5	<b>0.1165</b> (0.0164)	0.1834(0.0226)	0.1541(0.0177)	0.3107(0.0217)	0.3021(0.0213)
0.7	<b>0.1012</b> (0.0147)	0.1711(0.0218)	0.1551(0.0172)	0.3005(0.0216)	0.3054(0.0209)
0.9	<b>0.1084</b> (0.0152)	0.1725(0.0204)	0.1595(0.0171)	0.2927(0.0205)	0.2907(0.0198)

the performance of TS-2 appears to be better than TS-1, suggesting that converting a non-uniform hypergraph to a uniform one by adding null vertices can be a better data processing approach than decomposing a non-uniform hypergraph into a collection of uniform hypergraphs of different range. It is also interesting to note that HEM is fairly robust to the hypergraph network sparsity and the community imbalance, whereas the performance of other competing methods can be substantially affected.

To examine the network estimation accuracy, the averaged estimation errors of HEM, measured by  $n^{-m/2} \|\hat{\Theta} - \Theta^*\|_F$ , and their corresponding standard errors are reported in Table 3. Note that other competing methods solely focus on community detection, and thus do not produce estimate of  $\Theta^*$ . Clearly, the estimation error of HEM becomes smaller as the number of vertices increases, the network becomes denser or the communities become more balanced.

Table 3: The averaged estimation errors and their corresponding standard errors of HEM over 50 independent replications on the non-uniform hypergraph networks generated from Scenario 1 and 2.

Scenario 1	$s_n = 0.4$	0.2	0.1	0.05	0.025
$n = 300$	0.7165(0.1076)	0.7462(0.1076)	0.7207(0.0977)	0.8111(0.1174)	0.9436(0.1252)
400	0.7072(0.1080)	0.7192(0.1024)	0.7368(0.1048)	0.8182(0.1264)	0.9472(0.1504)
500	0.7301(0.1174)	0.6965(0.1152)	0.6820(0.1017)	0.7468(0.1196)	0.8027(0.1196)
Scenario 2	$\kappa_1/\kappa_2 = 0.1$	0.3	0.5	0.7	0.9
$n = 300$	1.2024(0.3076)	0.8646(0.1824)	0.8153(0.1585)	0.7316(0.1382)	0.7727(0.1221)

Finally, Figure 2 displays the first 15 eigenvalues of two randomly generated hypergraphs from Scenarios 1 and 2. It is clear that the first 2 leading singular values are substantially larger than the remaining singular values, confirming the choice of  $K = 2$  in the synthetic networks and the effectiveness of the eigen-gap approach.

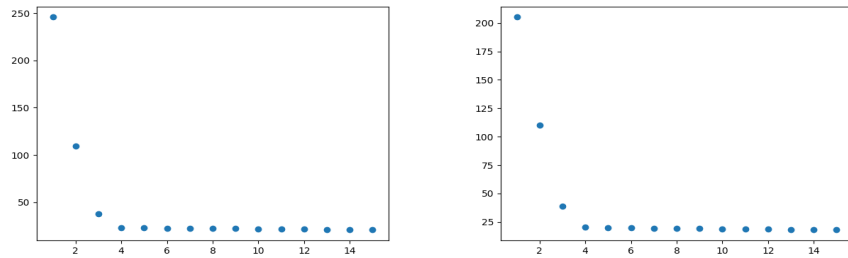


Figure 2: The first leading 15 singular values of a hypergraph network randomly generated from Scenario 1 (left) and Scenario 2 (right).

## 5.2 Two real-life hypergraph networks

We now apply the proposed HEM method to analyze two real-life hypergraph networks, including the Medical Subject Headings (MeSH) hypergraph network (Ke et al., 2021) and the cardiac Single Proton Emission Computed Tomography (SPECT) network (Dua and Graff, 2017).

The MeSH network is extracted from the MEDLINE database, which is available at <https://www.nlm.nih.gov/bsd/medline.html>. It consists of 318 MeSH terms of two diseases: Neoplasms (C04) and Nerve System Diseases (C10), which are represented as the vertices in the hypergraph network. The hyperedges are 10,472 papers published in 1960 where one or more of the above Mesh terms are annotated. After deleting the duplication hyperedges, there are a total of 1,375 hyperedges left, consisting of 297, 883, 174, 20 and 1 hyperedges of size 1, 2, 3, 4, and 5, respectively. We also remove those 21 hyperedges of size greater than 3 and all the hyperedges of size 1 due to their lack of information about latent community structure. After the pre-processing, we obtain a hypergraph of range 3 with 281 vertices and 1,057 hyperedges of size 2 or 3, where 180 vertices come from C04 and the other 101 vertices come from C10.

The SPECT network (<https://archive.ics.uci.edu/ml/datasets/spect+heart>) contains the SPECT images of 267 patients, where each image has been processed to 44 categorical fea-

tures to discriminate abnormal patients from the normal ones. To construct the hypergraph network, each patient is represented as a vertex, and for a possible value of each feature, we construct a hyperedge that contains all the patients sharing the particular feature value. Such a hypergraph construction method has been studied by Schölkopf et al. (2007) and Ghoshdastidar and Dukkipati (2017a). After deleting the replication hyperedges, there are a total of 1,483 hyperedges with sizes varying from 1 to 36. We only consider those hyperedges of size ranging from 2 to 6, and for hyperedges with sizes greater than 3, we convert them to all possible 3-cliques, leading to multiple hyperedges with size 3. Replication hyperedges and isolated vertices are further deleted. After the pre-processing, we obtain a hypergraph with 264 vertices and 2,950 hyperedges, where 211 vertices come from the abnormal patients and the other 53 ones come from the normal patients.

We perform different community detection methods on both hypergraph networks. As suggested in Ke et al. (2021), we set  $K = 6$  for the reg-HOOI algorithm in Tensor-SCORE, and thus we also set the embedding dimension  $r = 6$  in HEM for fair comparison. The network sparsity factor in HEM is estimated by hyperedge density; that is,  $s_n = 1057 \times \left(\binom{281}{2} + \binom{281}{3}\right)^{-1}$  in MeSH network and  $s_n = 2950 \times \left(\binom{264}{2} + \binom{264}{3}\right)^{-1}$  in SPECT network. The scaled Hamming errors of all the hypergraph community detection methods are reported in Table 4.

Table 4: Scaled Hamming errors of different hypergraph community detection methods on two real-life hypergraph networks.

	HEM	TS-1	TS-2	SHP	WPTG
MeSH	<b>0.0427</b>	0.0819	0.0925	0.0498	0.3630
SPECT	<b>0.1970</b>	0.3295	0.2159	0.3181	0.2652

It is evident that the scaled hamming errors of HEM are smaller than the other three competitors in both hypergraph networks, demonstrating its advantage in terms of community detection. We further visualize the estimated communities in both hypergraph networks

in Figure 3 by multidimensional scaling, where the community structures detected by HEM are very clear in the embedding space.

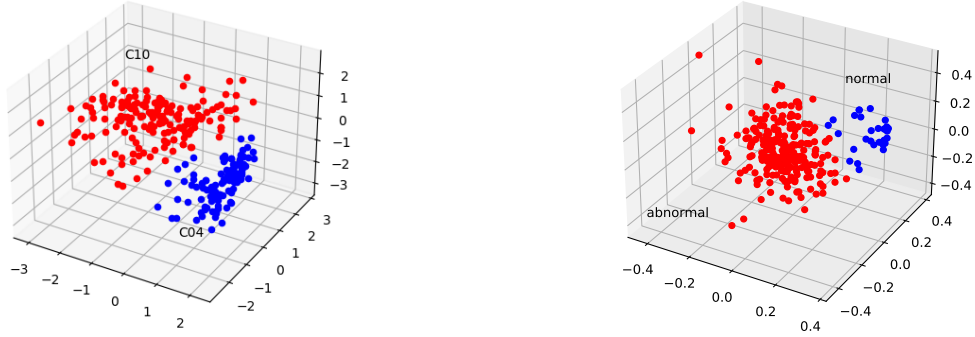


Figure 3: The detected communities in the embedding space of the MeSH hypergraph network (left) and the SPECT hypergraph network (right).

## 6 Conclusion

This article proposes a novel community detection method on general hypergraph networks. The proposed method is built upon a tensor-based hypergraph embedding model, which consists of a network augmentation step and an network embedding step. The resultant negative log-likelihood function is equipped with a new regularization term to encourage community structures among the embedding vectors. The proposed method is supported by various numerical experiments and asymptotic consistency in terms of community detection. Particularly, the theoretical results can be established for very sparse hypergraph network with link probability of order  $s_n \gg n^{1-m} \log n$ . It is worth pointing out that the proposed community detection method can be extended to various scenarios, such as multi-layer hypergraph networks or communities with mixed memberships, which is under further investigation.



## Acknowledgment

This research is supported in part by HK RGC Grants GRF-11303918, GRF-11300919, and GRF-11304520. We thank the associate editor and three anonymous referees, whose constructive comments and suggestions have led to significant improvements of the article. We also thank Dr. Dong Xia for sharing the MeSH dataset.

## References

- Agarwal, S., Lim, J., Zelnik-Manor, L., Perona, P., Kriegman, D., and Belongie, S. (2005). Beyond pairwise clustering. In *2005 IEEE Computer Society Conference on Computer Vision and Pattern Recognition (CVPR'05)*, volume 2, pages 838–845. IEEE.
- Ahn, K., Lee, K., and Suh, C. (2018). Hypergraph spectral clustering in the weighted stochastic block model. *IEEE Journal of Selected Topics in Signal Processing*, 12(5):959–974.
- Arous, G. B., Mei, S., Montanari, A., and Nica, M. (2019). The landscape of the spiked tensor model. *Communications on Pure and Applied Mathematics*, 72(11):2282–2330.
- Bahmanian, M. A. and Sajna, M. (2015). Connection and separation in hypergraphs. *Theory and Applications of Graphs*, 2(2):5.
- Chen, J. and Yuan, B. (2006). Detecting functional modules in the yeast protein–protein interaction network. *Bioinformatics*, 22(18):2283–2290.
- Chen, K. and Lei, J. (2018). Network cross-validation for determining the number of communities in network data. *Journal of the American Statistical Association*, 113(521):241–251.
- Chien, I. E., Lin, C.-Y., and Wang, I.-H. (2019). On the minimax misclassification ratio of hypergraph community detection. *IEEE Transactions on Information Theory*, 65(12):8095–8118.
- De Lathauwer, L., De Moor, B., and Vandewalle, J. (2000). A multilinear singular value decomposition. *SIAM Journal on Matrix Analysis and Applications*, 21(4):1253–1278.
- Dua, D. and Graff, C. (2017). UCI machine learning repository.
- Gallo, G., Longo, G., Pallottino, S., and Nguyen, S. (1993). Directed hypergraphs and applications. *Discrete Applied Mathematics*, 42(2):177 – 201.

- Ghoshdastidar, D. and Dukkipati, A. (2014). Consistency of spectral partitioning of uniform hypergraphs under planted partition model. In Ghahramani, Z., Welling, M., Cortes, C., Lawrence, N. D., and Weinberger, K. Q., editors, *Advances in Neural Information Processing Systems 27*, pages 397–405. Curran Associates, Inc.
- Ghoshdastidar, D. and Dukkipati, A. (2015a). A provable generalized tensor spectral method for uniform hypergraph partitioning. In *Proceedings of the 32nd International Conference on International Conference on Machine Learning - Volume 37*, ICML’15, page 400–409. JMLR.org.
- Ghoshdastidar, D. and Dukkipati, A. (2015b). Spectral clustering using multilinear svd: Analysis, approximations and applications. In *Proceedings of the Twenty-Ninth AAAI Conference on Artificial Intelligence*, AAAI’15, page 2610–2616. AAAI Press.
- Ghoshdastidar, D. and Dukkipati, A. (2017a). Consistency of spectral hypergraph partitioning under planted partition model. *The Annals of Statistics*, 45(1):289–315.
- Ghoshdastidar, D. and Dukkipati, A. (2017b). Uniform hypergraph partitioning: Provable tensor methods and sampling techniques. *Journal of Machine Learning Research*, 18(50):1–41.
- Hoff, P. D., Raftery, A. E., and Handcock, M. S. (2002). Latent space approaches to social network analysis. *Journal of the American Statistical Association*, 97(460):1090–1098.
- Ji, P., Jin, J., et al. (2016). Coauthorship and citation networks for statisticians. *The Annals of Applied Statistics*, 10(4):1779–1812.
- Jin, J. (2015). Fast community detection by score. *Ann. Statist.*, 43(1):57–89.
- Jing, B.-Y., Li, T., Lyu, Z., and Xia, D. (2021). Community detection on mixture multi-layer networks via regularized tensor decomposition. *arXiv preprint arXiv:2002.04457*.
- Ke, Z. T., Shi, F., and Xia, D. (2021). Community detection for hypergraph networks via regularized tensor power iteration. *arXiv preprint arXiv:1909.06503*.
- Kim, C., Bandeira, A. S., and Goemans, M. X. (2017). Community detection in hypergraphs, spiked tensor models, and sum-of-squares. In *2017 International Conference on Sampling Theory and Applications (SampTA)*, pages 124–128. IEEE.
- Kolda, T. G. and Bader, B. W. (2009). Tensor decompositions and applications. *SIAM Review*, 51:455–500.
- Kovačević, M. and Tan, V. Y. (2018). Codes in the space of multisets—coding for permutation channels with impairments. *IEEE Transactions on Information Theory*, 64(7):5156–5169.

- Kumar, T., Vaidyanathan, S., Ananthapadmanabhan, H., Parthasarathy, S., and Ravindran, B. (2021). Hypergraph clustering: a modularity maximization approach. *arXiv preprint arXiv:1812.10869*.
- Lee, J., Kim, D., and Chung, H. W. (2021). Hypergraph clustering in the weighted stochastic block model via convex relaxation of truncated mle. *arXiv preprint arXiv:2003.10038*.
- Lee, S. H., Magallanes, J. M., and Porter, M. A. (2017). Time-dependent community structure in legislation cosponsorship networks in the congress of the republic of peru. *Journal of Complex Networks*, 5(1):127–144.
- Lei, J., Chen, K., and Lynch, B. (2019). Consistent community detection in multi-layer network data. *Biometrika*, 107(1):61–73.
- Lei, J., Rinaldo, A., et al. (2015). Consistency of spectral clustering in stochastic block models. *Annals of Statistics*, 43(1):215–237.
- Li, T., Levina, E., and Zhu, J. (2020a). Rejoinder: ‘Network cross-validation by edge sampling’. *Biometrika*, 107(2):289–292.
- Li, X., Chen, Y., and Xu, J. (2020b). Convex relaxation methods for community detection. *arXiv preprint arXiv:1810.00315*.
- Loyal, J. D. and Chen, Y. (2020). Statistical network analysis: A review with applications to the coronavirus disease 2019 pandemic. *International Statistical Review*, 88(2):419–440.
- Nepusz, T., Yu, H., and Paccanaro, A. (2012). Detecting overlapping protein complexes in protein-protein interaction networks. *Nature methods*, 9(5):471.
- Newman, M. E., Watts, D. J., and Strogatz, S. H. (2002). Random graph models of social networks. *Proceedings of the National Academy of Sciences*, 99(suppl 1):2566–2572.
- Ouvrard, X., Goff, J.-M. L., and Marchand-Maillet, S. (2021). Adjacency and tensor representation in general hypergraphs part 1: e-adjacency tensor uniformisation using homogeneous polynomials. *arXiv preprint arXiv:1712.08189*.
- Pearson, K. J. and Zhang, T. (2014). On spectral hypergraph theory of the adjacency tensor. *Graphs and Combinatorics*, 30:1233–1248.
- Pearson, K. J. and Zhang, T. (2015). The laplacian tensor of a multi-hypergraph. *Discrete Mathematics*, 338(6):972 – 982.
- Qi, L. (2005). Eigenvalues of a real supersymmetric tensor. *Journal of Symbolic Computation*, 40(6):1302 – 1324.
- Robeva, E. (2016). Orthogonal decomposition of symmetric tensors. *SIAM Journal on Matrix Analysis and Applications*, 37(1):86–102.

- Schölkopf, B., Platt, J., and Hofmann, T. (2007). *Learning with Hypergraphs: Clustering, Classification, and Embedding*, pages 1601–1608. MITP.
- Sengupta, S. and Chen, Y. (2018). A block model for node popularity in networks with community structure. *Journal of the Royal Statistical Society: Series B (Statistical Methodology)*, 80(2):365–386.
- Sidiropoulos, N. D. and Bro, R. (2000). On the uniqueness of multilinear decomposition of n-way arrays. *Journal of Chemometrics: A Journal of the Chemometrics Society*, 14(3):229–239.
- Tang, X., Xue, F., and Qu, A. (2020). Individualized multi-directional variable selection.
- Tron, R. and Vidal, R. (2007). A benchmark for the comparison of 3-d motion segmentation algorithms. In *2007 IEEE conference on computer vision and pattern recognition*, pages 1–8. IEEE.
- Wang, J. (2010). Consistent selection of the number of clusters via crossvalidation. *Biometrika*, 97(4):893–904.
- Yuan, M., Liu, R., Feng, Y., and Shang, Z. (2021). Testing community structures for hypergraphs. *arXiv preprint arXiv:1810.04617*.
- Zhang, J., He, X., and Wang, J. (2021). Directed community detection with network embedding. *Journal of the American Statistical Association*, 0(0):1–11.
- Zhao, Y., Levina, E., and Zhu, J. (2011). Community extraction for social networks. *Proceedings of the National Academy of Sciences*, 108(18):7321–7326.
- Zhao, Y., Levina, E., Zhu, J., et al. (2012). Consistency of community detection in networks under degree-corrected stochastic block models. *The Annals of Statistics*, 40(4):2266–2292.